

# Heat Flux Variations over Sea Ice Observed at the Coastal Area of the Sejong Station, Antarctica

Sang-Jong Park, Tae-Jin Choi, and Seong-Joong Kim

Korea Polar Research Institute, Incheon, Korea

(Manuscript received 18 June 2012; revised 5 December 2012; accepted 20 December 2012)

© The Korean Meteorological Society and Springer 2013

**Abstract:** This study presents variations of sensible heat flux and latent heat flux over sea ice observed in 2011 from the 10-m flux tower located at the coast of the Sejong Station on King George Island, Antarctica. A period from July to September was selected as a sea ice period based on daily record of sea state and hourly photos looking at the Marian Cove in front of the Sejong Station. For the sea ice period, mean sensible heat flux is about  $-11 \text{ W m}^{-2}$ , latent heat flux is about  $+2 \text{ W m}^{-2}$ , net radiation is  $-12 \text{ W m}^{-2}$ , and residual energy is  $-3 \text{ W m}^{-2}$  with clear diurnal variations. Estimated mean values of surface exchange coefficients for momentum, heat and moisture are  $5.15 \times 10^{-3}$ ,  $1.19 \times 10^{-3}$ , and  $1.87 \times 10^{-3}$ , respectively. The observed exchange coefficients of heat shows clear diurnal variations while those of momentum and moisture do not show diurnal variation. The parameterized exchange coefficients of heat and moisture produces heat fluxes which compare well with the observed diurnal variations of heat fluxes.

**Key words:** Sea ice, heat flux, exchange coefficient, Sejong Station, Antarctica

## 1. Introduction

Since 1990s, many attentions are paid to the rapid decrease of the Arctic sea ice (Rorhrock *et al.*, 1999). Reduced Arctic sea ice extent impacts atmosphere-cryosphere-hydrosphere interactions causing regional and global climate changes (Serreze *et al.*, 2007; Liu *et al.*, 2012). In addition, opening of the Arctic Sea caused by Arctic warming is of great interest in economical, social, and diplomatic aspects to many of the northern hemispheric countries (Wadhams, 2012). Therefore, prediction of sea ice variation is now an impending topic to human beings.

To understand the variation of sea ice and associated energy budget in polar regions, we need to measure turbulent heat exchanges over sea ice. However, most of the past observations were short made at drifting station over sea ice (Thorpe *et al.*, 1973; Jordan *et al.*, 1999; Persson *et al.*, 2002; Muller *et al.*, 2012) or on airplane platform (Hartmann *et al.*, 1994). Long-term flux observations over sea ice would be beneficial to enhance our understanding of the heat flux variation over sea ice.

A good way to make long-term flux data is to measure fluxes at coastal regions at high latitudes near sea ice. With onshore winds, measured flux represents sea state and sea ice if the sea surface is frozen. In this study, flux data of the Sejong Station are analyzed as an example of heat exchange over sea ice. Located on King George Island of the Antarctic Peninsula, the Sejong Station ( $62^{\circ} 13'S$ ,  $58^{\circ} 47'W$ ) is surrounded by the Marian Cove and Maxwell Bay which were frozen from July to mid-October in 2011.

This study aims to show the heat flux variations and turbulent exchange characteristics over sea ice using eddy-covariance data produced at the Sejong Station. Section 2 provides site descriptions and data processing in detail and section 3 presents the heat flux variations and exchange coefficients related with air-sea ice heat exchange. Finally, summary and discussion are given in section 4.

## 2. Sejong Station and data

### a. Geographical environment

The Sejong Station is located on King George Island near the tip of the Antarctic Peninsula ( $62^{\circ} 13'S$ ,  $58^{\circ} 47'W$ ). The eddy covariance system is installed at 10-m flux tower which is 450 m away from the station. The flux tower sees the Marian Cove in the direction of from  $260^{\circ}$  to  $30^{\circ}$  and there is a low (120 m) hill across the Marian Cove 1.2 km away from the tower. The sea ice fetch in the direction of Maxwell Bay ( $260^{\circ}$  to  $315^{\circ}$ ) is more than 6 km and is over 1.2 km in the Marian Cove direction ( $315^{\circ}$  to  $0^{\circ}$ ) (Fig. 1). The flux tower looks land area in the south which is excluded in the present study. The distance from the flux tower to the shoreline is 10-20 m depending on the sea level.

According to the annual weather reports of Sejong Station from 1988 to 2011, the annual mean air temperature at 2 m a.g.l. is  $-1.7^{\circ}\text{C}$  with the lowest monthly air temperature of  $-5.6^{\circ}\text{C}$  in July. Minimum daily temperature record is  $-25.6^{\circ}\text{C}$  and maximum  $13.2^{\circ}\text{C}$  (Chae *et al.*, 2012). In 2011, annual mean air temperature was  $-2.8^{\circ}\text{C}$  (maximum  $9.4^{\circ}\text{C}$ , minimum  $-21.2^{\circ}\text{C}$ ) and wind speed at 10 m a.g.l. was  $8.2 \text{ m s}^{-1}$  (maximum wind gust  $41.2 \text{ m s}^{-1}$ ) with predominant wind direction of E or NW throughout the year. Annual mean relative humidity was 89%, cloud amount was 7.1 octa, annual precipitation amount was

Corresponding Author: Sang-Jong Park, Division of Polar Climate Research, Korea Polar Research Institute, 26 Songdomirae-ro, Yeosu-gu, Incheon 406-840, Korea.  
E-mail: sangjong@kopri.re.kr

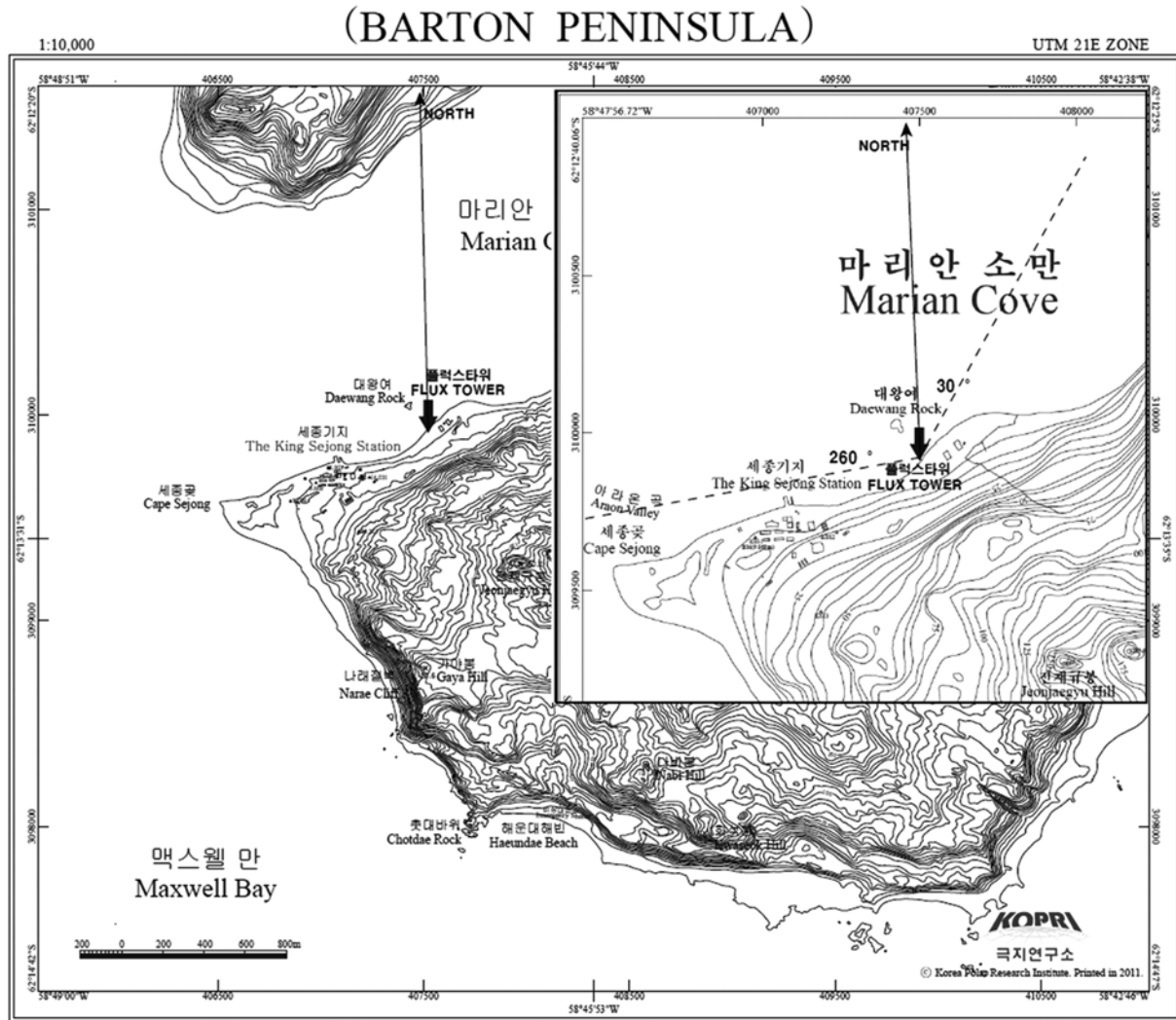


**Fig. 1.** Map showing the Sejong Station on King George Island, Antarctica. Location of the flux tower is marked with a thick arrow. Wind directions corresponding to sea ice fetch (from 260° to 30° clockwise) are shown in the inserted map.

581.5 mm, and annual occurrence number of blizzard was 27 (total duration time 248.8 hours).

From November to May, the Maxwell Bay and Marian Cove are usually open ocean frequently covered with drift ice along the shore. According to the annual weather report of the Sejong station in 2011, the Marian Cove had been covered by sea ice from June 29 to October 13 (Fig. 2).

**b. Measurement**

Turbulent flux at the coast of the Sejong Station has been measured since 2008 using a 10-m flux tower. Eddy covariance system is composed of a 3-D sonic anemometer (CSAT3, Campbell Scientific Inc.) and an open-path gas analyzer (LI-7500, LI-COR) measuring three dimensional wind, temperature, and water vapor at 20 Hz. Calibration of the gas analyzer has been performed once a year and the last calibration for the present data was conducted in December 2010. Four radiation

components (RLUP: upward longwave radiation, RLDN: downward longwave radiation, RSUP: upward shortwave radiation, RSDN: downward shortwave radiation) were obtained from a net radiometer (CNR1, Kipp & Zonen) at the flux tower. In addition, air temperature and humidity data were obtained from the automatic meteorological tower (AMOS-2) located about 60 m west of the Sejong station. More details of the meteorological instrumentation are given in Table 1. Besides above meteorological sensors, a camera took pictures of the Marian Cove every hour, which are useful to provide visual information on the sea ice condition.

**c. Data processing**

The sea ice period was determined based on the daily records in the annual weather report and the photos of the Marian Cove. Daily record contains the sea state information and the presence of sea ice in the Maxwell Bay and Marian



**Fig. 2.** Photos taken on January 14 (upper left), January 15 (upper right), June 30 (lower left), and August 14 (lower right) in 2011 looking at the Marian Cove from the Sejong Station. Flux tower is marked with arrow on the right-side of the photo.

**Table 1.** Description of meteorological variables observed at the Sejong Station.

Equipment	Variable	Manufacturer/Model	Height	Platform
Anemometer	3D wind and sonic temperature	Campbell/CSAT3	10 m	Flux tower
Open path gas analyzer	H <sub>2</sub> O and CO <sub>2</sub>	LiCOR/LI7500	10 m	Flux tower
Radiometer	Shortwave radiation Longwave radiation Net radiation	Kipp&Zonen/CNR1	2 m	Flux tower
Temperature and humidity probe	Air temperature/Relative humidity	Vaisala/HMP45D	2 m	AMOS2

Cove. Then, the hourly photos of Marian Cove were referenced to confirm the presence of sea ice. As a result, the “sea ice period” in this study was determined as 90 days from July through September.

The length of a typical 30-minute interval was used in the flux calculation. For data quality control, range check and spike check were applied (Vickers and Mahrt, 1997) and the trend in 30-minutes data was removed. Detrended wind data were rotated into mean wind direction (Kaimal and Finnigan, 1994) to calculate fluxes. Calculated sensible and latent heat fluxes went through flux corrections like sonic temperature correction (Schotanus *et al.*, 1983), frequency response correction (Moore, 1986), and density variation correction for latent heat flux (Webb *et al.*, 1980). Then additional data selection criteria such as diagnostic value of sonic anemometer and gas analyzer, precipitation, relative humidity, standard deviations of wind, sonic temperature, and humidity were also implemented to discard questionable flux data.

Finally, flux data were screened based on wind direction to select only on-shore winds. Specific criteria for each screening procedure are presented in Table 2. In short, from 4320 data points of 90-days, about 30% of sensible heat and latent heat flux data passed quality control processes.

Besides the sensible heat flux (SHF) and latent heat flux (LHF), surface exchange coefficients of momentum, heat, and moisture were estimated to analyze turbulent exchange process over sea ice.

$$SHF = \rho C_p C_h U (T_{sfc} - T) \quad (1a)$$

$$LHF = \rho (L_v + L_f) C_q U (Q_{sfc} - Q) \quad (1b)$$

where  $\rho$  is air density,  $C_p$  is the specific heat of air,  $U$  is wind speed,  $T_{sfc}$  is surface temperature,  $T$  is air temperature,  $L_v$  is the latent heat of vaporization,  $L_f$  is the latent heat of fusion,  $Q_{sfc}$  is surface specific humidity,  $Q$  is specific humidity. Here,  $Q_{sfc}$

**Table 2.** Criteria of flux data selection in this study.

Variable	Criteria
Wind speed	0~50 m s <sup>-1</sup>
Sonic temperature	-30~30°C
Water vapor	0~20 g m <sup>-3</sup>
Friction velocity	0.01~1.0 m s <sup>-1</sup>
Heat flux (sensible, latent each)	± 100 W m <sup>-2</sup>
Sonic diagnostic value	< 3
Maximum AGC (LI-7500)	65%
Precipitation	0 mm
Relative humidity	< 97%
Surface energy residual (Rnet - (SHF + LHF))	< 50 W m <sup>-2</sup>
Standard deviation (stdev) of vertical wind	< 2 m s <sup>-1</sup>
Stdev of H <sub>2</sub> O	< 2 g m <sup>-3</sup>
Stdev of sonic temperature	< 1.5°C
Wind direction	On-shore (260°~30°)

was calculated assuming saturated with respect to ice at the surface temperature  $T_{sfc}$  (Persson *et al.*, 2002).

Surface temperature ( $T_{sfc}$ ) was calculated using the longwave radiation data as below.

$$T_{sfc} = [\{RLUP - (1 - \varepsilon)RLDN\} / \varepsilon\sigma]^{1/4} \quad (2)$$

where  $RLUP$  and  $RLDN$  are upward and downward longwave radiations, respectively;  $\varepsilon$  is longwave emissivity of the surface, and  $\sigma$  is the Stefan-Boltzman constant. In this study, the emissivity ( $\varepsilon$ ) of 0.99 was chosen for snow and ice surfaces (Grenfell *et al.*, 1998; Persson *et al.*, 2002). This study assumes that upward longwave radiation from the snow surface near the flux tower is practically equivalent to those over sea ice. As an effort to reduce uncertainty in exchange coefficient stemming from gradient measurement, we discarded exchange coefficient if gradient is less than a criteria. We decided temperature criteria as 0.5°C considering temperature sensor error (< 0.3°C) and  $T_{sfc}$  uncertainty (0.2°C) and humidity criteria as 0.15 g kg<sup>-1</sup> which is about two times of 2% of measured humidity. Here,  $T_{sfc}$  uncertainty is estimated as a mean difference between  $T_{sfc}$  values using a range of snow/ice emissivity ( $\varepsilon = 0.95 \sim 0.99$ ) in previous studies.

Along with the observed turbulent exchange coefficients, parameterized  $C_h$  and  $C_q$  were estimated as in Eq. (3) to validate against the observed values in Eqs. (1a) and (1b).

$$C_x = \frac{k^2}{\left\{ \ln\left(\frac{z-d}{z_{0m}}\right) - \Psi_m\left(\frac{z-d}{L}\right) \right\} \left\{ \ln\left(\frac{z-d}{z_{0x}}\right) - \Psi_x\left(\frac{z-d}{L}\right) \right\}} \quad (3)$$

Here,  $\Psi_m$  and  $\Psi_x$  are stability correction functions for mo-

**Table 3.** Empirical coefficients for scalar roughness lengths in the relationship of  $\ln(z_{0x}/z_{0m}) = b_0 + b_1 \ln(Re_*) + b_2 (\ln(Re_*))^2$ .

	Smooth ( $Re_* \leq 0.135$ )	Transition ( $0.135 < Re_* < 2.5$ )	Rough ( $2.5 \leq Re_* < 1000$ )
Heat	$b_0 = 1.250$ $b_1 = 0.000$ $b_2 = 0.000$	$b_0 = 0.149$ $b_1 = -0.550$ $b_2 = 0.000$	$b_0 = 0.317$ $b_1 = -0.565$ $b_2 = -0.183$
Moisture	$b_0 = 1.610$ $b_1 = 0.000$ $b_2 = 0.000$	$b_0 = 0.351$ $b_1 = -0.628$ $b_2 = 0.000$	$b_0 = 0.396$ $b_1 = -0.512$ $b_2 = -0.180$

mentum and scalar, respectively,  $k$  is the von-Karman constant (= 0.4),  $d$  is displacement height, and  $L$  is the Monin-Obkhov length scale. The stability correction functions of Dyer (1974) and Beljaars and Holtslag (1991) were chosen for unstable and stable conditions, respectively. Stability functions for heat was used for moisture for simplicity. Scalar roughness lengths of heat ( $z_{0h}$ ) and moisture ( $z_{0q}$ ) in Eq. (3) were calculated following the parameterization of Andreas (1987), who related the ratio of roughness lengths of scalar and momentum with the roughness Reynolds number. That is to say,  $\ln(z_{0x}/z_{0m})$  in Eq. (4), where  $x$  represents scalar such as heat ( $h$ ) and moisture ( $q$ ), is parameterized as a function of  $Re_*$  ( $= z_{0m} u_* v^{-1}$ , where  $u_*$  is the friction velocity and  $v$  is the kinematic viscosity of air) as

$$\ln(z_{0x}/z_{0m}) = b_0 + b_1 \ln(Re_*) + b_2 \ln^2(Re_*) \quad (4)$$

where,  $b_0$ ,  $b_1$ ,  $b_2$  are empirical coefficients depending on the flow status and the scalar quantity (Table 3).

Prior to the  $z_{0x}$  calculation, momentum roughness length ( $z_{0m}$ ) was estimated from the wind profile relationship of

$$U = \frac{u_*}{k} \left\{ \ln\left(\frac{z-d}{z_{0m}}\right) - \Psi_m\left(\frac{z-d}{L}\right) + \Psi_m\left(\frac{z_{0m}}{L}\right) \right\}, \quad (5)$$

where  $U$  is the wind speed at 10 m height;  $z$  is the measurement height;  $d$  is the zero-plane displacement height;  $\Psi_m$  is the stability correction function; and  $L$  is the Monin-Obukhov length scale. The displacement height  $d$  is set to zero in this study because it is presumably negligible compared to the height  $z$  over snow and ice. Then, with  $z_{0m}$  and  $u_*$ , roughness Reynolds number ( $Re_*$ ) is calculated to yield the ratio ( $z_{0x}/z_{0m}$ ). The estimated  $z_{0x}$  is used to produce  $C_x$  and then to parameterize heat flux as in Eq. (1).

### 3. Results

#### a. Weather and heat flux

As stated in Section 2a, the sea surface had been covered with sea ice from 29 July to 13 October in 2011. Figure 3 presents heat flux and relevant meteorological data in August 2011. During the month, the air temperature fluctuates between -20°C and 0°C and the surface temperature is generally lower than the air temperature by 1-2°C. Downward shortwave

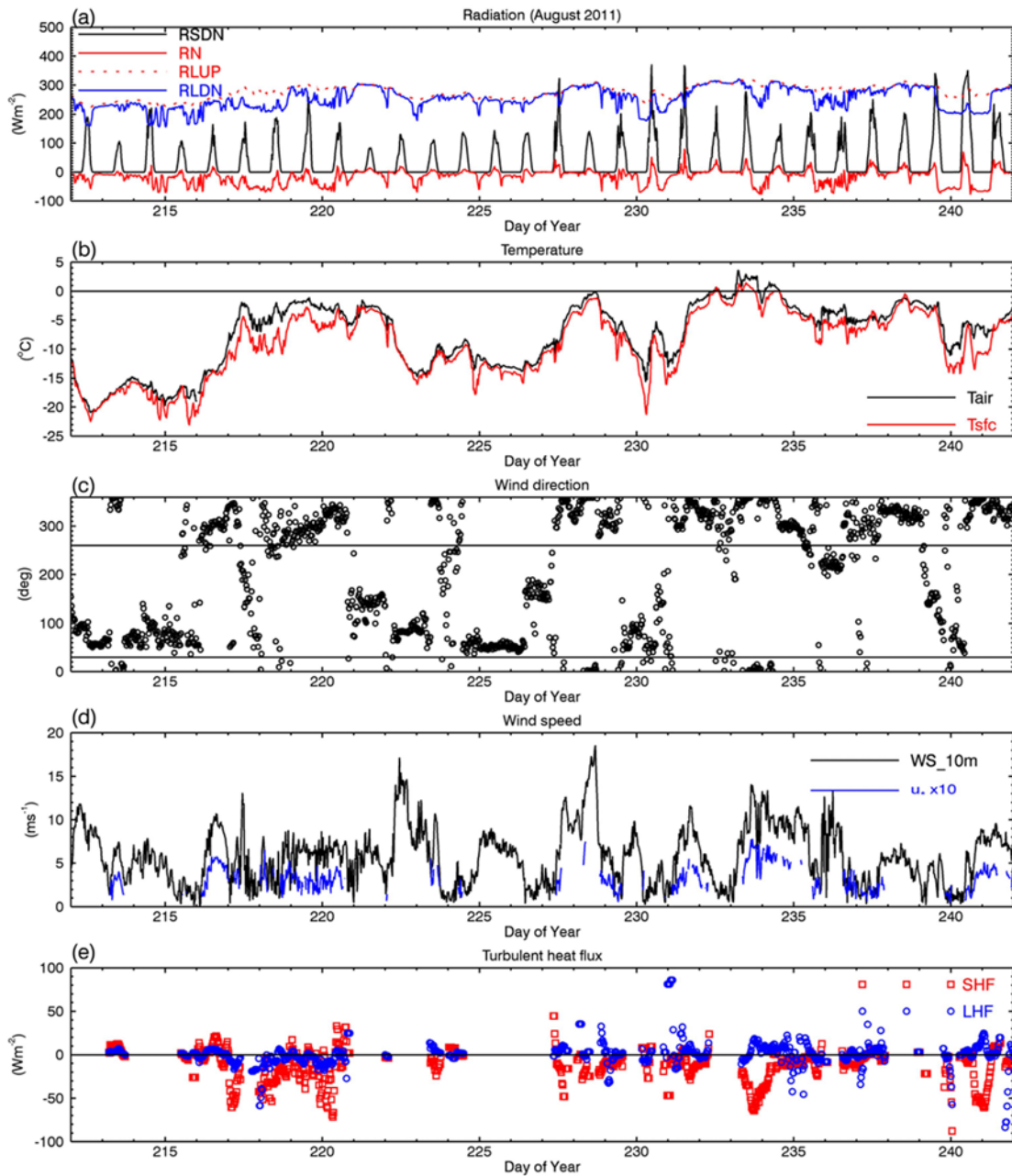


**Fig. 3.** Variations of meteorological variables in August 2011: (a) downward solar radiation ( $RSDN$ ), downward longwave radiation ( $RLDN$ ), upward longwave radiation ( $RLUP$ ), and net radiation ( $RN$ ), (b) air temperature ( $T_{air}$ ) and surface temperature ( $T_{sc}$ ), (c) wind direction, (d) wind speed ( $WS_{10m}$ ) and friction velocity ( $u^*$ ), and (e) sensible heat flux ( $SHF$ ) and latent heat flux ( $LHF$ ). Note the horizontal lines in (c) are drawn to mark on-shore wind directions ( $WD < 30^{\circ}$  or  $WD > 260^{\circ}$ ).

radiation during daytime increases with time over  $100 \text{ W m}^{-2}$  but due to the high albedo of snow and sea ice surface net radiation is mostly negative showing radiative cooling of surface. The magnitudes of sensible and latent heat fluxes are usually less than  $50 \text{ W m}^{-2}$  even during daytime. Majority of the sensible heat flux is negative meaning downward heat transfer from the atmosphere to the sea ice agreeing with the temperature difference between air and sea ice surface. However, the latent heat flux is in many cases upward implying

moisture supply from the sea ice surface to the overlying atmosphere.

Considering small magnitude and fluctuation of direction of LHF, it seems that vapor pressure in the atmosphere and saturation vapor pressure at the sea ice surface are of similar magnitudes so that LHF responds sensitively to the humidity or surface temperature. This implies that small bias in temperature or humidity of sea ice surface and overlying air can make modeled LHF fluctuates sensitively over sea ice.

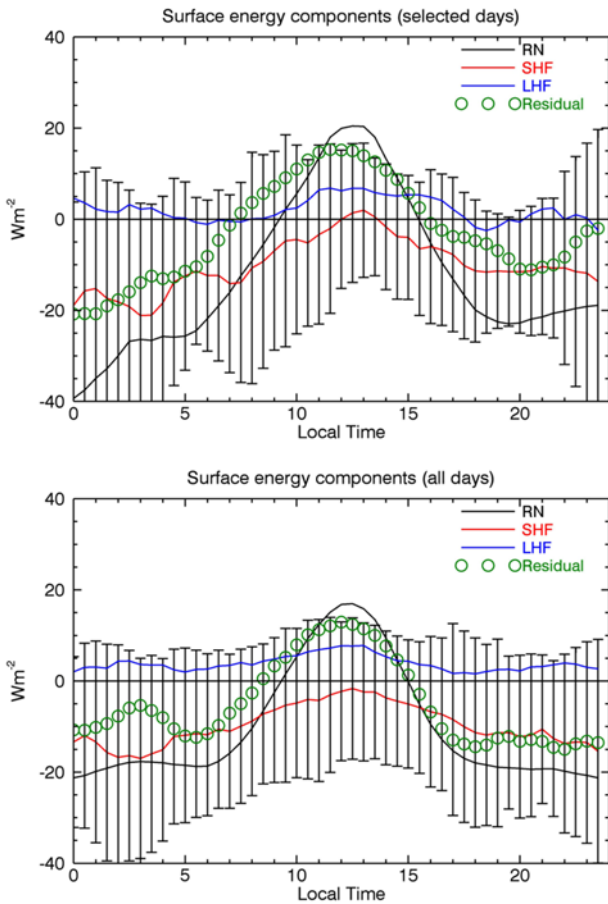


**Fig. 4.** Mean diurnal variations of net radiation (*RN*), sensible heat flux (*SHF*), latent heat flux (*LHF*), and residual energy (*Residual*). Standard errors for *SHF* are shown together. Upper panel shows the average over the selected 13-days with over 2/3 times valid data a day and lower panel shows the average over whole 90-days of sea ice period. Note that positive *RN* and *Residual* mean downward while positive *SHF* and *LHF* are upward.

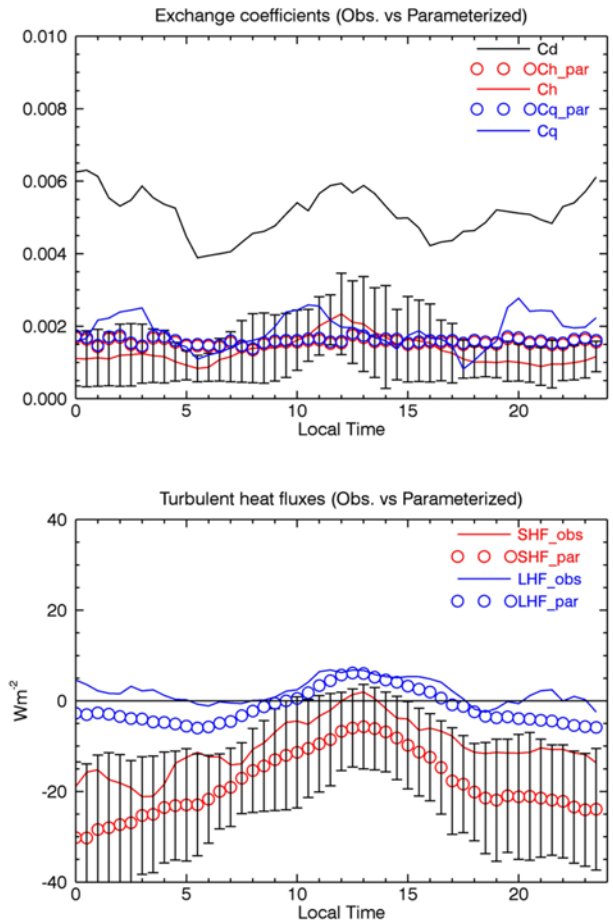
**b. Diurnal variations of heat flux**

Figure 4 shows the mean diurnal variations of heat fluxes and net radiation for the sea ice period averaged over selected 13 days with over 2/3 times of valid data each day. Net radiation is negative with mean value of  $-12 \text{ W m}^{-2}$  meaning radiative cooling of the surface. The downward sensible heat flux is largest during nighttime and smallest at noon with the daily mean value of about  $-11 \text{ W m}^{-2}$ . Despite some negative values during nighttime, the daily mean latent heat flux is  $+2 \text{ W m}^{-2}$  because of the positive heat flux during daytime. Assuming energy balance at the sea ice surface, the residual energy ( $-3 \text{ W m}^{-2}$ ) indicates that this amount of heat should be transferred upward from the sea ice bottom to the surface.

Mean values of energy components using all available data from the 90 days and the 13 days of the sea ice period are given in Table 4. Among previous studies on the heat flux over sea ice, SHEBA (Surface Heat Budget of the Arctic Ocean Experiment) data are compared to the present results. In the

**Table 4.** Mean values of energy fluxes for the sea ice period (unit:  $\text{W m}^{-2}$ ).

	Selected 13-days	All 90-days
Sensible heat flux	$-10.7 (\pm 21.4)$	$-10.1 (\pm 20.7)$
Latent heat flux	$+1.9 (\pm 16.0)$	$+3.3 (\pm 15.8)$
Net radiation	$-12.2 (\pm 26.6)$	$-10.0 (\pm 27.0)$
Residual	$-2.7 (\pm 23.0)$	$-3.9 (\pm 23.3)$



**Fig. 5.** (Upper) Mean diurnal variations of surface exchange coefficients of momentum ( $C_d$ ) and sensible heat ( $C_h$ ) and moisture ( $C_q$ ) averaged over the selected 13-days. Standard errors for  $C_h$  (upper panel) and  $SHF_{par}$  (lower panel) are shown, respectively. Note that the parameterized  $C_h$  ( $C_{h,par}$ ) and  $C_q$  ( $C_{q,par}$ ) are nearly the same. (lower) Mean diurnal variations of the observed ( $SHF_{obs}$ ,  $LHF_{obs}$ ) and parameterized heat fluxes ( $SHF_{par}$  and  $LHF_{par}$ ).

SHEBA project, which had been conducted for one year over multi-year pack ice in the Arctic Ocean, monthly mean sensible heat flux during wintertime (December, January, and February) was about  $-7 \text{ W m}^{-2}$  and latent heat flux was also negative with small magnitude of being less than  $1 \text{ W m}^{-2}$ . The conductive heat transfer calculated from the surface temperature and snow-ice interface temperature was about  $-5 \text{ W m}^{-2}$  during wintertime (Persson *et al.*, 2002). This indicates that the mean values of sensible heat flux ( $-11 \text{ W m}^{-2}$ ), latent heat flux

( $+2 \text{ W m}^{-2}$ ), and residual energy ( $-3 \text{ W m}^{-2}$ ) in this study obtained from the Antarctic sea ice compare very well with the SHEBA result from the Arctic sea ice.

### c. Surface exchange coefficients and parameterized heat fluxes

Figure 5 shows the mean diurnal variations of surface exchange coefficients calculated from the observed fluxes in parallel with the parameterized results using the equations of Andreas (1987) as well as the calculated heat fluxes using parameterized exchange coefficients of heat and moisture. It is found that mean  $C_d$  is about  $5.15 \times 10^{-3}$  while  $C_h$  and  $C_q$  are about  $1.19 \times 10^{-3}$  and  $1.87 \times 10^{-3}$  which are about a quarter and one-third of  $C_p$ , respectively. It is noted that observational  $C_h$  shows distinct diurnal variation unlike  $C_d$  and  $C_q$ . The simulated  $C_h$  and  $C_q$  do not show any distinct variation with time. The parameterized sensible heat flux is distinctively downward most of time with mean values of  $-18.8 \text{ W m}^{-2}$ . Meanwhile, the parameterized latent heat flux shows upward transfer during daytime and slight downward transfer during nighttime with mean value of  $-1.6 \text{ W m}^{-2}$ . Overall, the parameterized heat fluxes show similar magnitude of diurnal variation but with some biases. And it is found that the diurnal variation of the parameterized heat fluxes is mainly determined by the diurnal variation of temperature and humidity differences rather than the exchange coefficient variation.

## 4. Summary and discussions

Eddy covariance data obtained from a 10-m tower at coastal area of the Sejong Station in 2011 were analyzed to examine variation of heat fluxes over sea ice. Annual weather report and hourly photos of the Marian Cove were used for determination of the sea ice period as July through September. Data screening based on various quality control criteria yielded about 30% of data for the final analysis. The mean sensible heat flux is about  $-11 \text{ W m}^{-2}$ , latent heat flux is about  $+2 \text{ W m}^{-2}$ , and residual energy is  $-3 \text{ W m}^{-2}$ . In the presence of sea ice, sensible heat flux is usually downward while latent heat flux is on average upward with downward values during nighttime. Estimated mean values of surface exchange coefficients for momentum, heat and moisture are  $5.15 \times 10^{-3}$ ,  $1.19 \times 10^{-3}$ , and  $1.87 \times 10^{-3}$ , respectively. The observed exchange coefficients of heat shows clear diurnal variations while those of momentum and moisture do not show diurnal variation.

Heat fluxes in the present study agree well with the winter-time heat fluxes of the SHEBA data obtained over the Arctic sea ice. Temporal variation of radiation and surface temperature indicate that a decrease of downward longwave radiation causes a decrease of net radiation at the surface and then surface temperature due to radiative cooling. Changes of surface temperature consequently would alter the air-sea ice heat flux by changing air-sea ice temperature and humidity gradient. Braun *et al.* (2001) suggested that large-scale circulation is critical to heat flux over land. In the case of the Sejong Station,

air mass change implied by a change of downward longwave radiation seems to influence heat fluxes over sea ice.

Previous studies suggested that heat exchange between sea ice and underlying sea-water is important in sea ice energy budget (Gordon, 1981; Woodgate *et al.*, 2010). If we assume energy balance to be closed at the sea ice surface, the residual energy ( $-3 \text{ W m}^{-2}$ ) in this study should be balanced with the upward heat flux from the sea ice bottom. Sea ice temperature data to estimate heat transfer through sea ice is not available for the present study. Our assumption that  $T_{sfc}$  calculated using the longwave radiation data over snow surface next to the flux tower is equivalent to the true surface temperature of the sea ice upwind of the flux tower needs to be validated in the future when sea ice temperature data are available. In fact, counter-gradient sensible heat flux data in some cases and biases in the parameterized sensible heat flux and latent heat flux might be explained if there is a bias between the surface temperature calculated with the longwave radiation data next to the tower and the true sea ice surface temperature.

Along with sea ice temperature, sea ice depth is also very important in the sea ice-related energy exchange validation. The depth of sea ice can be used to estimate heat flux between the top and bottom of sea ice so that it enables us to measure or estimate every component of energy balance at the sea ice surface. Moreover, temporal variation of sea ice depth is required to validate sea ice prediction which results from our current knowledge of sea ice-related energy exchanges.

The characteristics of turbulent exchange are presented in terms of exchange coefficients of heat and moisture. It is interesting that the observed exchange coefficient of heat shows clear diurnal variation while the parameterized coefficient remains nearly constant all day. Still, the parameterized heat fluxes agree very well with the observed heat fluxes including the diurnal variations except some bias. The feasible reasons for the discrepancy in diurnal variations of exchange coefficients and heat fluxes between the observed and parameterized require further analysis.

The flux data of the Sejong Station are valuable to monitor heat flux variation over sea ice because the station is at coastal region with a wide view of sea, and flux measurement can be carried out throughout a year regardless of sea ice condition. Further analysis using the Sejong Station flux data would enhance our understanding of atmosphere-sea ice interaction and sea ice variations in polar regions.

**Acknowledgements.** This study has been supported by the research project ‘Reconstruction and Observation of Components for Southern and Northern Annular Mode to Investigate the Cause of Polar Climate Change (PE13010)’ of Korea Polar Research Institute. We would like to thank Byung-Gil Lee and Jung-Ock Son of Korea Polar Research Institute for their help in measurement and analysis of the data. The authors also appreciate two anonymous reviewers for their helpful opinions to improve this manuscript.

Edited by: Jong-Jin Baik

## REFERENCES

- Andreas, E. L., 1987: A theory for the scalar roughness and the scalar transfer coefficients over snow and sea ice. *Bound.-Layer Meteor.*, **38**, 159-184.
- Beljaars, A. C. M., and A. A. M. Holtslag, 1991: On flux parameterization over land surfaces for atmospheric models. *J. Appl. Meteorol.*, **30**, 327-341.
- Braun, M., H. Saurer, G. Vogt, J. C. Simoes, and H. Gobmann, 2001: The influence of large-scale atmospheric circulation on the surface energy balance of the King George Island ice cap. *Int. J. Climatol.*, **21**, 21-36.
- Chae, N. Y., B. Y. Lee, Y. J. Yoon, T. J. Choi, S. J. Park, J. K. Park, and B. G. Lee, 2012: Annual weather report Antarctic King Sejong Station, 2011, Korea Polar Research Institute.
- Choi, T., B. Y. Lee, H.-C. Lee, and J.-S. Shim, 2004: Surface flux measurements at King Sejong Station in West Antarctica, I. Turbulent characteristics and sensible heat flux. *Ocean and Polar Research*, **26**, 453-463.
- \_\_\_\_\_, Lee, B.-Y., Kim, S.-J., Yoon, Y.-J., and Lee, H.-C., 2008: Net radiation and turbulent energy exchanges over a non-glaciated coastal area on King George Island during four summer seasons. *Antarctic Science*, **20**(1), 99-111.
- Dyer, A. J., 1974: A review of flux-profile relationships. *Bound.-Layer Meteor.*, **7**, 363-372.
- Foken, T., and B. Wichura, 1996: Tools for quality assessment of surface-based flux measurements. *Agric. Forest Meteorol.*, **78**, 83-105.
- Grenfell *et al.*, 1998: Evolution of electromagnetic signatures of sea ice from initial formation to the establishment of thick first-year ice. *IEEE Trans. Geosci. Remote Sens.*, **36**, 1642-1654.
- Gordon, A. L., 1981: Seasonality of Southern Ocean Sea Ice, *J. Geophys. Res.*, **86**(C5), 4193-4197, doi:10.1029/JC086iC05p04193.
- Hartmann, J., C. Kottmeier, C. Wamser, and E. Augstein, 1994: Aircraft measured atmospheric momentum, heat and radiation fluxes over Arctic sea ice, Geophysical Monograph Series. *The Polar Oceans and Their Role in Shaping the Global Environment*, **85**, 443, doi:10.1029/GM085p0443.
- Jordan, R. E., E. L. Andreas, and A. P. Makshtas, 1999: Heat budget of snow-covered sea ice at North Pole 4. *J. Geophys. Res.*, **104**(C4), 7785-7806, doi:10.1029/1999JC900011.
- Kaimal, J. and J. J. Finnigan, 1994: *Atmospheric Boundary Layer Flows-their structure and measurement*. Oxford University Press, 289 pp.
- Liu, J., J. A. Curry, H. Wang, M. Song, and R. M. Horton, 2012: Impact of declining Arctic sea ice on winter snowfall. *Proc. Natl. Acad. Sci.*, **109**(11), 4074-4079, doi:10.1073/pnas.1114910109.
- Moore, C. J., 1986: Response corrections for eddy correlation systems. *Bound.-Layer Meteor.*, **37**(1-2), 17-35.
- Muller, J. B. A., J. R. Dorsey, M. Flynn, M. W. Gallagher, C. J. Percival, D. E. Shallcross, A. Archibald, H. K. Roscoe, R. W. Obbard, and H. M. Atkinson, 2012: Energy and ozone fluxes over sea ice. *Atmos. Environ.*, **47**, 218.
- Persson, P. O. G., C. W. Fairall, E. L. Andreas, P. S. Guest, and D. K. Perovich, 2002: Measurements near the Atmospheric Surface Flux Group tower at SHEBA: Near-surface conditions and surface energy budget. *J. Geophys. Res.*, **107**(C10), 8045, doi:10.1029/2000JC000705.
- Rothrock, D. A., Y. Yu, and G. A. Maykut, 1999: Thinning of the Arctic sea ice cover. *Geophys. Res. Lett.*, **26**(23), 3469-3472, doi:10.1029/1999GL010863.
- Schotanus, P., F. T. M. Nieuwstadt, and H. A. R. DeBruin, 1983: Temperature measurement with a sonic anemometer and its application to heat and moisture fluctuations., *Bound.-Layer Meteor.*, **26**, 81-93.
- Serreze, M. C., M. M. Holland, and J. Stroeve, 2007: Perspectives on the Arctic's shrinking sea ice cover. *Science*, **315**(5818), 1533-1536, doi:10.1126/science.1139426.
- Thorpe, M. R., E. G. Banke, and S. D. Smith, 1973: Eddy correlation measurements of evaporation and sensible heat flux over Arctic sea ice., *J. Geophys. Res.*, **78**(18), 3573-3584, doi:10.1029/JC078i018p03573.
- Vickers, D., and L. Mahrt, 1997: Quality control and flux sampling problems for tower and aircraft data. *J. Atmos. Oceanic Technol.*, **14**, 512-526.
- Wadhams, P., 2012: Arctic ice cover, ice thickness and tipping points. *AMBIO: J. Human Environ.*, **41**(1), 23-33, doi:10.1007/s13280-011-0222-9.
- Webb, E. K., G. I. Pearman, and R. Leuning, 1980: Correction of Flux Measurements for Density Effects Due to Heat and Water Vapour Transfer. *Quart. J. Roy. Meteor. Soc.*, **106**, 85-100.
- Woodgate, R. A., T. Weingartner, and R. Lindsay, 2010: The 2007 Bering Strait oceanic heat flux and anomalous Arctic sea ice retreat. *Geophys. Res. Lett.*, **37**, L01602, doi:10.1029/2009GL041621.